ISSN 1063-7761, Journal of Experimental and Theoretical Physics, 2014, Vol. 118, No. 4, pp. 501–511. © Pleiades Publishing, Inc., 2014.
Original Russian Text © M.V. Shevelev, A.S. Konkov, 2014, published in Zhurnal Eksperimental'noi i Teoreticheskoi Fiziki, 2014, Vol. 145, No. 4, pp. 579–590.

ATOMS, MOLECULES, OPTICS

Peculiarities of the Generation of Vavilov–Cherenkov Radiation Induced by a Charged Particle Moving Past a Dielectric Target

M. V. Shevelev* and A. S. Konkov**

Tomsk Polytechnic University, Tomsk, 634050 Russia

**e-mail: mvshev@tpu.ru*

***e-mail: ekwinus@tpu.ru*

Received May 13, 2013

Abstract—We consider Vavilov–Cherenkov radiation occurring as a result of uniform motion of a point charge in vacuum near a finite-size prismatic target with an arbitrary permittivity. The expression derived for the spectral-angular density of radiation contains a center of emission of Vavilov–Cherenkov radiation, which depends on the angle of flight of the point charge relative to the target. The results indicate that the main contribution to the formation of Vavilov–Cherenkov radiation comes from the polarization current occurring at the interface between the media.

DOI: 10.1134/S1063776114030182

1. INTRODUCTION

The essence of the Vavilov–Cherenkov effect is that an electric charge moving in a medium at a constant velocity emits electromagnetic waves with a continuous spectrum and specific angular distribution. Radiation is emitted only if the velocity of the charge exceeds the phase velocity of light in the transparent medium under investigation. A specific feature of the angular distribution is that wavevector $\mathbf{k}$ of emitted waves forms angle Θ with velocity $\mathbf{v}$, such that $n\beta\cos\Theta = 1$, where n is the refractive index of the transparent medium. In 1947, Frank and Ginzburg [1] considered radiation generated by a charge moving uniformly along the axis of a cylindrical channel cut through in a medium with permittivity ε_1 and filled with a substance having permittivity ε_2. This problem is important because energy losses for Vavilov–Cherenkov radiation (VCR) as a charge moves in a medium are comparatively small (these are mainly ionization losses localized in the immediate vicinity of the trajectory). For this reason, ionization losses are avoided for motion in channels, slits, and in the vicinity of the medium, and VCR is preserved. In recent years, intense studies have been carried out in the field of nondestructive testing of relativistic beams [2–7] and for developing new methods of accelerating charged particles [8, 9] based on VCR generated by short bunches of charged particles in the vicinity of finite-size targets.

It should be noted that there are very few exact solutions to the VCR problem for media with sharp boundaries. The most important exactly solvable problems are the above-mentioned problem of emission of radiation by a charge uniformly moving along the axis of a cylindrical channel [1, 10] and the problem of radiation occurring when a charged particle moves through a sphere [11] or past a periodic structure consisting of spherical targets with a finite conductivity [12]. Solving such problems in more complex geometries is hampered due to the difficulties in formulating the boundary conditions.

In [13], the characteristics of transition radiation from perfectly conducting focusing targets were investigated with a method in which polarization radiation is considered as the field of the current induced on a target surface by the field of a point charge moving uniformly along a straight line. This method was subsequently generalized in [14–16] for media with finite conductivity and dimensions. The polarization current method was used in [15] to solve the problem of radiation occurring as a charge moves along the axis of a cylindrical vacuum channel in a finite-radius screen. Depending on the parameters, the resulting solution describes various types of radiation (transition radiation, VCR, and diffraction radiation). In the case of a transparent medium, the solution completely coincides with the analytic expression obtained in the Cherenkov radiation theory for a finite-thickness layer [17]; for a thicker layer, the solution gives the well-known Tamm–Frank formula for VCR in an unbounded transparent medium. The advantages of this method lie in the possibility of determining the characteristics of various types of polarization radiation for targets with complex surface profiles with allowance for the actual electric dielectric properties of the material.

This article is devoted to application of the polarization current method to solving the problem of VCR occurring from the uniform motion of a point charge in vacuum in the vicinity of a finite-size prismatic tar-

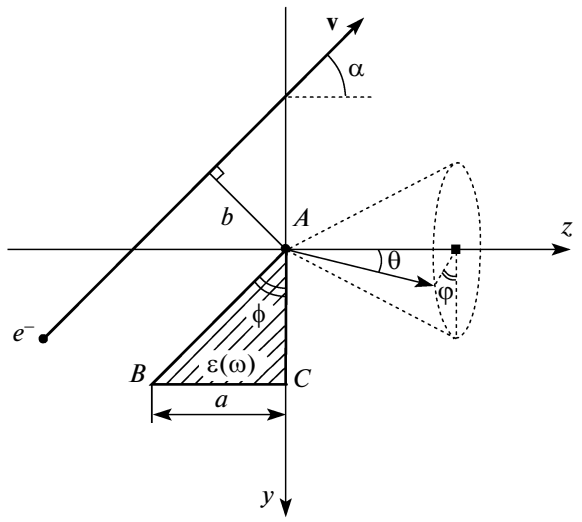

Fig. 1. Diagram of generation of polarization radiation by a charged particle moving uniformly near a prismatic wedge.

get with an arbitrary permittivity and to analysis of peculiarities of the radiation field.

2. VAVILOV–CHERENKOV RADIATION FROM A DIELECTRIC WEDGE

VCR is polarization radiation emitted by atoms of a medium under the action of external field $\mathbf{E}^0$ of a particle with energy

$$\gamma = \frac{E}{mc^2} = \frac{1}{\sqrt{1-\beta^2}},$$

which moves at a constant velocity $v = \beta c$ in the substance (or near it). Therefore, the radiation field is a solution to the "vacuum" macroscopic Maxwell equations with the polarization current on the right-hand side, the density of which for a nonmagnetic medium has the form

$$\mathbf{j}_{\text{pol}} = \sigma(\omega)(\mathbf{E}^0 + \mathbf{E}^{\text{pol}}(\mathbf{j}_{\text{pol}})), \quad (1)$$

where $\mathbf{E}^0 \equiv \mathbf{E}^0(\mathbf{r}, \omega)$ and $\mathbf{E}^{\text{pol}} \equiv \mathbf{E}^{\text{pol}}(\mathbf{r}, \omega)$ are the Fourier transforms of the particle field in vacuum and of the field of the currents induced in the substance, respectively. Conductivity $\sigma(\omega)$ of the medium appearing in Eq. (1) is related to permittivity $\varepsilon(\omega)$ of the medium by the well-known relation

$$\sigma(\omega) = \frac{i\omega}{4\pi}(1-\varepsilon(\omega)). \quad (2)$$

Maxwell's equations lead to the following equation for the magnetic field $\mathbf{H}^{\text{pol}}$ of polarization radiation:

$$\left(\Delta + \varepsilon(\omega)\frac{\omega^2}{c^2}\right)\mathbf{H}^{\text{pol}}(\mathbf{r}, \omega) = -\frac{4\pi}{c}\sigma(\omega)\text{curl}\,\mathbf{E}^0(\mathbf{r}, \omega). \quad (3)$$

The solution to the this equation in the wave zone gives the field of polarization radiation emitted by atoms and molecules of the substance under the action of the field of the particle as a result of so-called distant collisions, in which the energy lost by the particle is negligibly small as compared to the total energy.

If the polarization currents are induced in a limited volume (i.e., the medium has boundaries), integration in the solution to Eq. (3) is performed only over volume V_T occupied by the currents:

$$\mathbf{H}^{\text{pol}}(\mathbf{r}, \omega) = \text{curl}\frac{1}{c}\int_{V_T}\sigma(\omega)\mathbf{E}^0(\mathbf{r}', \omega) \times \frac{\exp(i\sqrt{\varepsilon(\omega)}|\mathbf{r}'-\mathbf{r}|\omega/c)}{|\mathbf{r}'-\mathbf{r}|}d^3r'. \quad (4)$$

It should be noted that this expression is the exact solution to the Maxwell equations, which makes it possible to avoid solving differential equation (1). Allowance for the second term on the right-hand side of Eq. (1) would ultimately lead to replacement of vacuum wavenumber ω/c by $\sqrt{\varepsilon(\omega)}\,\omega/c$. Such a replacement describes the "renormalization" of the field of the charge in the medium due to the contribution from the field of the polarization current [15]. In spite of its comparative simplicity, this expression describes all types of polarization radiation generated in the medium with an arbitrary conductivity and an arbitrary inhomogeneity (i.e., in a target of any shape).

Let us use this method in the problem of radiation occurring as a result of uniform motion of a charged particle in vacuum in the vicinity of a finite-size prismatic target with an arbitrary permittivity (Fig. 1).

Since the target in Fig. 1 is assumed to be infinitely large only along the x axis, expression (4) used for determining the strength of the magnetic field of radiation should be written in the form

$$\mathbf{H}^{\text{pol}}(\mathbf{r}, \omega) = \frac{2\pi i}{c}\frac{\exp[i\omega\sqrt{\varepsilon}r/c]}{r}\mathbf{q}\int_{-a}^{0}dz' \times \int_{-z'\cot\phi}^{a\cot\phi}\sigma(\omega)\mathbf{E}^0(q_x, y', z', \omega)e^{-q_y y'}e^{-q_z z'}dy', \quad (5)$$

where $\mathbf{q} = (\omega/c)\sqrt{\varepsilon}\,\mathbf{e}$ is the wavevector and $\mathbf{e} = \mathbf{r}/r$.

The Fourier component of the particle field appearing in expression (5) can be determined from the total Fourier transform of the field:

$$\mathbf{E}^0(\mathbf{q}, \omega) = \frac{4\pi i}{\omega}\frac{\mathbf{j}^0(\mathbf{q}, \omega)\omega^2/c^2 - \mathbf{q}(\mathbf{q}\cdot\mathbf{j}^0(\mathbf{q}, \omega))}{\mathbf{q}^2 - \omega^2/c^2}. \quad (6)$$

The Fourier transform of the current density produced by the charge moving along an oblique trajectory in the geometry shown in Fig. 1 has the form

$$\mathbf{j}^0(\mathbf{q},\omega) = \frac{e\mathbf{v}}{(2\pi)^3}\delta(\mathbf{q}\cdot\mathbf{v}-\omega)\exp(iq_y h), \qquad (7)$$

where e is the particle charge, $\mathbf{v} = v\{0, -\sin\alpha, \cos\alpha\}$ is the velocity vector, $\delta(\mathbf{q}\cdot\mathbf{v}-\omega)$ is the Dirac delta function, and $h = b/\cos\alpha$.

Then, we can determine the Fourier component of the field of a particle moving uniformly at an angle to the target surface from the total Fourier component (6) of the field:

$$\mathbf{E}^0(q_x, y, z, \omega) = -\frac{ie}{2\pi v^2\sqrt{1+(\gamma\beta e_x)^2\varepsilon}}$$

$$\times\left\{\gamma\beta v e_x\sqrt{\varepsilon}, \gamma^{-1}v_y + i\,\mathrm{sgn}\left(y' - \frac{v_y}{v_z}z' + h\right)\right.$$

$$\times v_z\sqrt{1+(\gamma\beta e_x)^2\varepsilon},$$

$$\left.\gamma^{-1}v_z - i\,\mathrm{sgn}\left(y' - \frac{v_y}{v_z}z' + h\right)v_y\sqrt{1+(\gamma\beta e_x)^2\varepsilon}\right\} \qquad (8)$$

$$\times\exp\left[i\frac{\omega}{v_z}z'\right]\exp\left[i\frac{v_y\omega}{v^2}\left(y' - \frac{v_y}{v_z}z' + h\right)\right]$$

$$\times\exp\left[-\mathrm{sgn}\left(y' - \frac{v_y}{v_z}z' + h\right)\right.$$

$$\left.\times\frac{v_z\omega}{v^2\gamma}\sqrt{1+(\gamma\beta e_x)^2\varepsilon}\left(y' - \frac{v_y}{v_z}z' + h\right)\right].$$

Here, function $\mathrm{sgn}(y' - (v_y/v_z)z' + h)$ assumes a value of $+1$ if the target lies below the particle trajectory and -1 if the target lies above the particle trajectory.

Substituting expression (8) into formula (5), we can obtain the following expression for the radiation field in the medium:

$$\mathbf{H}^{\mathrm{pol}}(\mathbf{r},\omega) = \frac{e\beta\sqrt{\varepsilon}(\varepsilon-1)\mathbf{F}}{4\pi c\sqrt{1+(\gamma\beta e_x)^2\varepsilon}}\frac{\exp[i\omega\sqrt{\varepsilon}r/c]}{r}\left(\frac{1-\exp\left[-ia\frac{\omega}{v}(\cos\alpha-\beta\sqrt{\varepsilon}e_z+i\gamma^{-1}\sin\alpha\sqrt{1+(\gamma\beta e_x)^2\varepsilon})\right]}{\cos\alpha-\beta\sqrt{\varepsilon}e_z+i\gamma^{-1}\sin\alpha\sqrt{1+(\gamma\beta e_x)^2\varepsilon}}\right.$$

$$\left.+\frac{\exp\left[-ia\frac{\omega}{v}(\cos\alpha-\beta\sqrt{\varepsilon}e_z+i\gamma^{-1}\sin\alpha\sqrt{1+(\gamma\beta e_x)^2\varepsilon})\right]-\exp\left[ia\frac{\omega}{v}\cot\phi(\sin\alpha+\beta\sqrt{\varepsilon}e_y-i\gamma^{-1}\cos\alpha\sqrt{1+(\gamma\beta e_x)^2\varepsilon})\right]}{\cot\phi(\sin\alpha+\beta\sqrt{\varepsilon}e_y-i\gamma^{-1}\cos\alpha\sqrt{1+(\gamma\beta e_x)^2\varepsilon})+\cos\alpha-\beta\sqrt{\varepsilon}e_z+i\gamma^{-1}\sin\alpha\sqrt{1+(\gamma\beta e_x)^2\varepsilon}}\right) \qquad (9)$$

$$\times\frac{\exp\left[-\frac{\omega}{\gamma v}(h+a\cot\phi)\cos\sqrt{1+(\gamma\beta e_x)^2\varepsilon}\right]}{\gamma^{-1}\cos\alpha\sqrt{1+(\gamma\beta e_x)^2\varepsilon}+i\sin\alpha+i\beta\sqrt{\varepsilon}e_y}\exp\left[-ih\frac{\omega}{v}\sin\alpha\right]\exp\left[-i\frac{\omega}{v}a\cot\phi(\sin\alpha+\beta\sqrt{\varepsilon}e_y)\right],$$

where we have used the notation

$$\mathbf{F} = \left\{(\gamma^{-1}\cos\alpha + i\sin\alpha\sqrt{1+(\gamma\beta e_x)^2\varepsilon})e_y\right.$$

$$+(\gamma^{-1}\sin\alpha - i\cos\alpha\sqrt{1+(\gamma\beta e_x)^2\varepsilon})e_z,$$

$$(\gamma\beta\sqrt{\varepsilon}e_z - \gamma^{-1}\cos\alpha - i\sin\alpha\sqrt{1+(\gamma\beta e_x)^2\varepsilon})e_x,$$

$$\left.(i\cos\alpha\sqrt{1+(\gamma\beta e_x)^2\varepsilon} - \gamma^{-1}\sin\alpha - \gamma\beta\sqrt{\varepsilon}e_y)e_x\right\}.$$

In expression (9), we have taken into account the fact the target lies below the trajectory of the particle, i.e.,

$$\mathrm{sgn}\left(y' - \frac{v_y}{v_z}z' + h\right) = +1$$

(see Fig. 1). This expression defines the total radiation field in the medium. The components of vector $\mathbf{e}$ appearing in expression (9) can be written in terms of polar angle Θ in the medium:

$$\mathbf{e}\{\sin\Theta\sin\varphi, \sin\Theta\cos\varphi, \cos\Theta\}.$$

To find the radiation field in vacuum, we cannot directly use the Fresnel diffraction laws; for example, for good conductors, emitting dipoles are concentrated near the interface, and the field near the surface does not correspond to the wave zone. For this purpose, we can use the reciprocity theorem [18]

$$\left|\mathbf{E}^{\mathrm{pol(vac)}}\right| = \left|\frac{\sin\Theta}{\sin\theta}\mathbf{E}^{\mathrm{pol}(m)}\right|$$

$$= \left|\frac{1}{\sqrt{\varepsilon}}\mathbf{E}^{\mathrm{pol}(m)}\right| = \frac{1}{|\varepsilon|^2}\left|\mathbf{H}^{\mathrm{pol}(m)}\right|, \qquad (10)$$

where $\mathbf{E}^{\mathrm{pol(vac)}}$ is the sought radiation field in vacuum, which is produced by a dipole located in the medium, and $\mathbf{E}^{\mathrm{pol}(m)}$ is the radiation field in the medium, which is produced by the same dipole, but located in vacuum at a considerable distance from the interface. To connect the "vacuum" angle θ with angle Θ in the

medium, we used Snell's law in expression (10). Like in the formulation of the reciprocity theorem (10), we have taken into account the relationship between the strengths of the electric and magnetic fields in vacuum for a spherical wave:

$$\left|\mathbf{E}^{\mathrm{pol}(m)}\right| = \frac{1}{\sqrt{\varepsilon}}\left|\mathbf{H}^{\mathrm{pol}(m)}\right|.$$

To determine the electric field in vacuum in the case when the field of the wave incident on the interface from vacuum is defined by formula (10), the magnetic field strength in the medium should be decomposed into components relative to the plane of incidence of the wave:

$$\left|\mathbf{H}^{\mathrm{pol}(m)}\right|^2 = \left|H_{\parallel}^{\mathrm{pol}(m)}\right|^2 + \left|H_{\perp}^{\mathrm{pol}(m)}\right|^2,$$

where

$$\left|H_{\perp}^{\mathrm{pol}(m)}\right|^2 = \left|f_H\right|^2\left|H_{\perp}^{\mathrm{pol}}\right|^2,$$
$$\left|H_{\parallel}^{\mathrm{pol}(m)}\right|^2 = \left|\sqrt{\varepsilon}f_E\right|^2\left|H_{\parallel}^{\mathrm{pol}}\right|^2.$$

Consequently, the electric field strength in vacuum is defined by the formula

$$\left|\mathbf{E}^{\mathrm{pol(vac)}}\right|^2 = \frac{1}{|\varepsilon|^2} \times \left(\left|f_H\right|^2\left|H_{\perp}^{\mathrm{pol}}\right|^2 + \left|\sqrt{\varepsilon}f_E\right|^2\left|H_{\parallel}^{\mathrm{pol}}\right|^2\right). \quad (11)$$

Here, the following notation has been introduced: the components of magnetic field (9),

$$H_{\perp}^{\mathrm{pol}} = H_x^{\mathrm{pol}}\cos\varphi - H_y^{\mathrm{pol}}\sin\varphi,$$
$$H_{\parallel}^{\mathrm{pol}} = \sqrt{\left(H_z^{\mathrm{pol}}\right)^2 + \left(H_x^{\mathrm{pol}}\sin\varphi + H_y^{\mathrm{pol}}\cos\varphi\right)^2}, \quad (12)$$

which are perpendicular and parallel to the plane of incidence of the wave on the interface, as well as Fresnel coefficients

$$f_H = \frac{2\varepsilon\cos\theta}{\varepsilon\cos\theta + \sqrt{\varepsilon - \sin^2\theta}},$$
$$f_E = \frac{2\cos\theta}{\cos\theta + \sqrt{\varepsilon - \sin^2\theta}} \quad (13)$$

for an infinitely large interface. To find the radiation intensity in vacuum using expression (11), we must express the radiation angles in the medium in terms of corresponding radiation angles in vacuum:

$$e = \{\sin\Theta\sin\varphi, \sin\Theta\cos\varphi, \cos\Theta\} = \frac{1}{\sqrt{\varepsilon}}\left\{\sin\theta\sin\varphi, \sin\theta\cos\varphi, \sqrt{\varepsilon - \sin^2\theta}\right\}. \quad (14)$$

Thus, the spectral-angular density of polarized radiation can be determined from the relation

$$\frac{d^2W}{d\omega d\Omega} = cr^2\left|\mathbf{E}^{\mathrm{pol(vac)}}\right|^2 = \frac{cr^2}{|\varepsilon|^2}\left(\left|f_H\right|^2\left|H_{\perp}^{\mathrm{pol}}\right|^2 + \left|\sqrt{\varepsilon}f_E\right|^2\left|H_{\parallel}^{\mathrm{pol}}\right|^2\right). \quad (15)$$

Expression (15) for the spectral-angular distribution of polarized radiation was obtained by attaching the angles of observation to the Cartesian system of coordinates related to the target (see Fig. 1), which is unusual for such problems because in analyzing VCR, the radiation angles are normally measured from direction of the particle momentum. For this reason, we pass to the system of observation from the trajectory of a charged particle, in which the relation between angles θ and θ' can be written as $\theta = \theta' - \alpha$. We focus on the fact that for $\theta' > \alpha$, the azimuthal angle $\varphi = 0$, while for $\theta' < \alpha$, azimuthal angle $\varphi = \pi$ (see Fig. 1).

In experiments, it is often easier to rotate the target relative to the trajectory of the bunch of charged particles than to change the direction of the bunch; therefore, the relation between the angle of particle flight, the wedge angle, and the angle of rotation of the target can be written as $\alpha = \pi/2 - \phi - \psi$ (Fig. 2).

Consequently, the spectral-angular distribution of polarized radiation in the "forward" direction (positive direction of the z axis) has the form

$$\frac{d^2W}{d\omega d\Omega} = \frac{e^2\beta^2}{4\pi^2 c}\frac{\cos^2(\theta'-\alpha)}{|P|^2}\left|\frac{\varepsilon-1}{\varepsilon}\right|^2\left|1 - \frac{P\exp\left[i\frac{\omega}{\beta c}\Sigma a\cot\phi\right] + \Sigma\cot\phi\exp\left[-ia\frac{\omega}{\beta c}P\right]}{P + \Sigma\cot\phi}\right|^2$$
$$\times\left\{\left|\frac{\varepsilon}{\varepsilon\cos(\theta'-\alpha) + \sqrt{\varepsilon - \sin^2(\theta'-\alpha)}}\right|^2\left|\cos\alpha(\gamma^{-1}\sin(\theta'-\alpha) - iK\cos\varphi\sqrt{\varepsilon - \sin^2(\theta'-\alpha)})\right.\right.$$
$$\left.\left. + \sin\alpha(iK\sin(\theta'-\alpha) + \gamma^{-1}\cos\varphi\sqrt{\varepsilon - \sin^2(\theta'-\alpha)}) - \gamma\beta\sin(\theta'-\alpha)\sqrt{\varepsilon - \sin^2(\theta'-\alpha)}\sin^2\varphi\right|^2\right.$$
$$\left. + \left|\frac{\sqrt{\varepsilon}}{\cos(\theta'-\alpha) + \sqrt{\varepsilon - \sin^2(\theta'-\alpha)}}\right|^2(\gamma\sin\varphi)^2(\sin^2(\theta'-\alpha) + \left|\sqrt{\varepsilon - \sin^2(\theta'-\alpha)}\right|^2)\right\} \quad (16)$$

$$\times [1-\beta^2\cos^2(\theta'-\alpha)+2\beta\gamma^{-2}\sin\alpha\sin(\theta'-\alpha)\cos\varphi-\gamma^{-2}\sin^2\alpha(K^2-\gamma^{-2})]\Big\}$$

$$\times\frac{\exp\left[-2\frac{\omega}{\gamma\beta c}(h+a\cot\phi)K\cos\alpha\right]}{K^2(1-\beta^2\cos^2(\theta'-\alpha)+\beta^2\sin^2\alpha[1-\sin^2(\theta'-\alpha)\sin^2\varphi]+2\beta\sin\alpha\cos\varphi\sin(\theta'-\alpha))},$$

where the following notation has been introduced:

$$P = \cos\alpha-\beta\sqrt{\varepsilon-\sin^2(\theta'-\alpha)}+i\gamma^{-1}K\sin\alpha,$$

$$\Sigma = \sin\alpha+\beta\cos\varphi\sin(\theta'-\alpha)-i\gamma^{-1}K\cos\alpha,$$

$$K = \sqrt{1+(\gamma\beta\sin(\theta'-\alpha)\sin\varphi)^2}.$$

The expression derived for the spectral-angular density of polarization radiation takes into account both diffraction radiation (DR) and VCR, which corresponds to the pole in the denominator:

$$\left|\cos\alpha-\beta\sqrt{\varepsilon-\sin^2(\theta'-\alpha)}+i\gamma^{-1}K\sin\alpha\right|\longrightarrow 0.$$

For $\alpha\longrightarrow 0$, this expression passes to the well-known Vavilov–Cherenkov condition written in vacuum variables. However, for $\alpha\neq 0$, the VCR peak in the angular distribution is shifted. It should be noted that expression (16) also contains an extra VCR pole ensuring the displacement of polarization radiation peaks depending on the geometry of the chosen target, which in the given case is characterized by prism angle ϕ. Therefore, even when we consider the flight of a charged particle at angle $\alpha=0$ (see Fig. 1), the VCR peak will be displaced relative to the emission angles satisfying the well-known condition of generation of this radiation in the medium.

It should be noted that expression (16) derived above is valid only for angles of particle flight smaller than the critical angle α_{cr}; a further increase in the angle leads to the situation in which the particle trajectory intersects the target (Fig. 3) and, hence, to the generation of transient radiation in addition to diffraction radiation and VCR. The value of the critical angle is determined by the flight geometry of the charged particle and the target size from the following simple relation:

$$\alpha_{cr} = \arcsin\left(\frac{b}{a/\sin\phi}\right)+\frac{\pi}{2}-\phi.$$

The target geometry also imposes natural constraints on the result. To preserve the triangular profile of the prism, the prism angle must satisfy the condition $0<\phi<\pi/2$. Another limitation appears as a result of application of Fresnel coefficients (13) in the model for a planar infinitely large interface. This approximation is valid if the target parameter $a/\tan\phi$ considerably exceeds the wavelength of emitted radiation (i.e., when the condition $a/\tan\phi\gg\lambda$ is satisfied). In this case, face AC of the prism (see Fig. 1) through which radiation that propagateds to a vacuum can be assumed infinitely large compared to the radiation

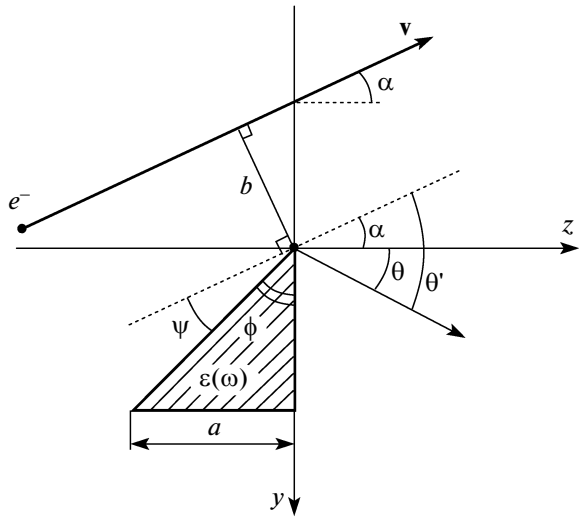

Fig. 2. Diagram illustrating a transition to new angles of observation and rotation of the target relative to the trajectory of a charged particle.

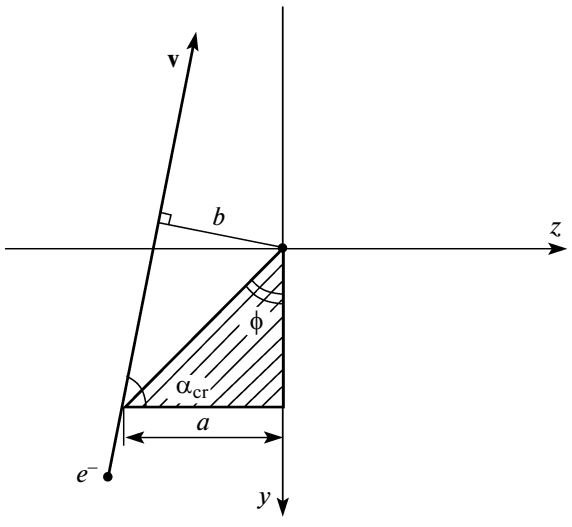

Fig. 3. Diagram of generation of polarization radiation by a charged particle moving at the critical angle towards a prismatic wedge.

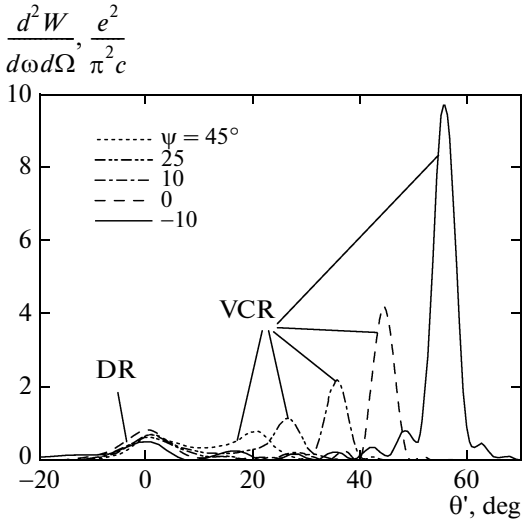

Fig. 4. Angular distribution of polarization radiation generated by a charged particle with energy $\gamma = 12$ moving near a dielectric wedge. Parameters are $\sqrt{\varepsilon} = 1.41$, $b = 15$ mm, $\phi = \pi/4$, $a = 45$ mm, and $\lambda = 4$ mm.

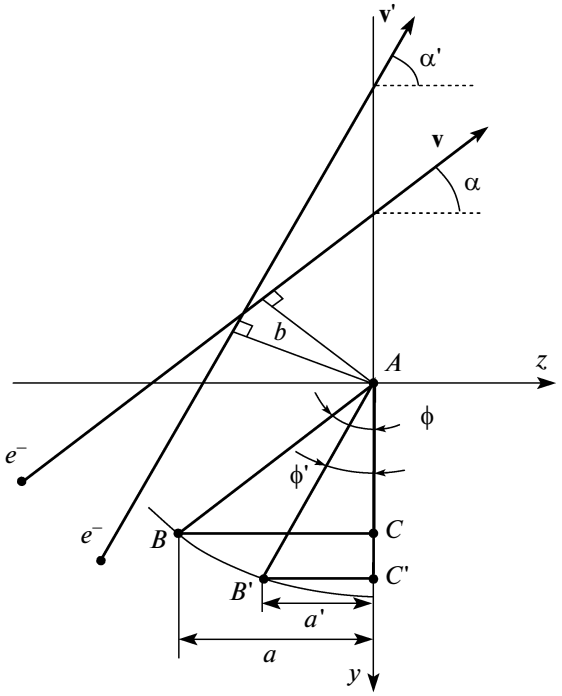

Fig. 5. Diagram of generation of polarization radiation illustrating the variation of the target volume upon a change in the vertex angle of the prismatic wedge.

wavelength, and the contribution from the edges can be disregarded.

Let us consider some features of polarization radiation for an oblique flight of a charged particle in the vicinity of a dielectric wedge. For a transparent substance satisfying the Vavilov–Cherenkov condition, the DR intensity is small, and the main contribution comes from Cherenkov radiation (Fig. 4). The DR intensity remains almost constant, and DR propagation corresponds to the direction of motion of the charged particle. With increasing flight angle α, the intensity at the VCR peak increases because the effective impact parameter decreases. The case in which rotation angle ψ is zero corresponds to parallel flight of the charged particle along the *AB* face; in this case, the direction of propagation of VCR satisfies the well-known relation $n\beta\cos\Theta = 1$ with allowance for the refraction of radiation at the output face *AC*. It should be noted once again that when rotation angle ψ of the target increases or decreases, the VCR propagation direction does not obey the requirements of the well-known Cherenkov relation. Pay attention to the chosen parameters of calculation, the results of which are shown in Fig. 4: the values of the charged particle energy, the permittivity of the target material, basic sizes, and the target geometry were selected in conformity with the experimental conditions for verifying our results.

To explain the effect of displacement of the VCR distribution peak, let us consider the dependence of the radiation peak intensity on the volume of the prismatic target.

Expression (16) makes it possible to explain the spectral-angular density of polarization radiation from prismatic targets of different volumes by varying angle ϕ and the vertex of the prismatic target (Fig. 5), thus changing its volume involved in the process of polarization by the charged particle. In all further calculations, we will consider only the flight of a charged particle parallel to face *AB* of the prismatic target; therefore, the relation between flight angle α and wedge angle ϕ assumes the form $\phi + \alpha = \pi/2$. In the traditional representation, the VCR intensity at the peak of the angular distribution is proportional to the squared mean free path of the charged particle in the medium; therefore, the size of the *AB* face of the prismatic target (from the side of motion of the charged particle) remains unchanged; consequently, quantity a in expression (16) can be written in the form $a = AB\sin\phi$.

The spectral-angular distribution of polarization radiation in the case when the particle trajectory is parallel to the target ($\phi = \pi/4$) with the angles attached to the system of coordinates is shown in Fig. 6. The radiation peak at $\theta_{ChR} = -0.73°$ indicates that VCR propagates at right angles to the *AC* face; therefore, the Fresnel coefficients make the smallest contribution to scattering and refraction of radiation occurring from the target material.

Let us analyze the dependence of radiation intensity at the peak of its angular distribution on the wedge angle ϕ and, hence, on wedge thickness a (Fig. 7).

It can be seen from Fig. 7 that upon a change in wedge angle ϕ, the VCR intensity at the angular distribution peak decreases. It should be noted that polar angle θ for VCR propagation in vacuum also varies

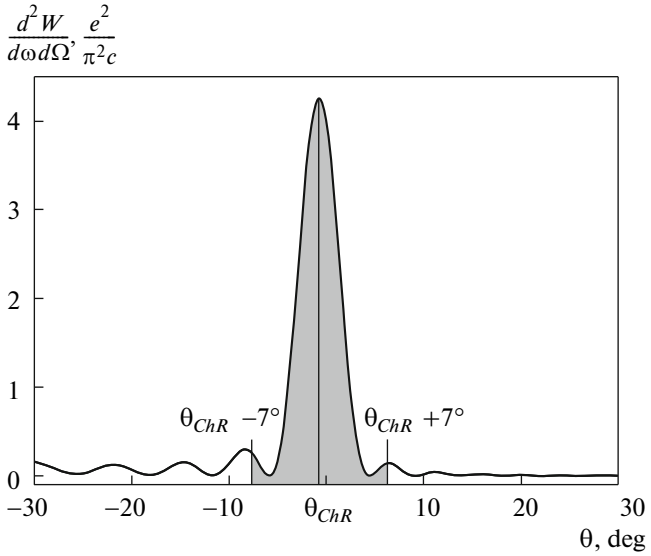

Fig. 6. Angular distribution of polarization radiation generated by a charged particle with energy $\gamma = 12$ flying along an oblique trajectory past a dielectric wedge. Parameters are $\sqrt{\varepsilon} = 1.41$, $b = 15$ mm, $l = 45\sqrt{2}$ mm, $\phi = \pi/4$, and $\lambda = 4$ mm.

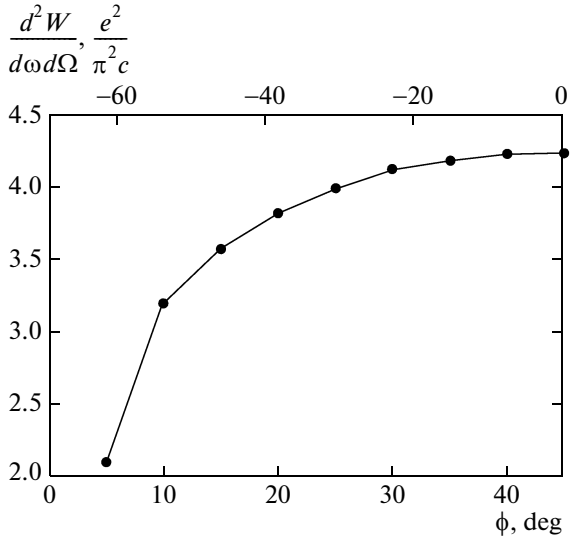

Fig. 7. Dependence of the VCR intensity at the angular distribution peak on wedge angle ϕ. Parameters are $\gamma = 12$, $\sqrt{\varepsilon} = 1.41$, $b = 15$ mm, $l = 45\sqrt{2}$ mm, and $\lambda = 4$ mm.

from zero (see Fig. 7); therefore, the Fresnel coefficients make a noticeable contribution to scattering of radiation passing from the target material to vacuum. Consequently, to take into account the total contribution from VCR to the spectral-angular distribution of polarization radiation, we must evaluate the integral over the entire area occupied by the VCR peak (Fig. 8):

$$S = \int\limits_{\theta_{ChR}-7^\circ}^{\theta_{ChR}+7^\circ} \frac{d^2W}{d\omega d\Omega} d\theta.$$

Comparing the results depicted in Figs. 7 and 8, we see that the total radiation intensity is independent of the thickness of the dielectric target. The effect under investigation can be explained, first, by the decrease in the field of the charged particle with increasing distance from its trajectory. Second, VCR is coherent radiation; consequently, constructive interference of radiation can take place only in a thin layer of the substance. It should be noted that the effect of VCR generation in the surface layer of the target was demonstrated experimentally for the first time in [19], where the disappearance of Cherenkov radiation was observed during investigation of simultaneous generation of diffraction radiation and Cherenkov radiation in a dielectric target after the installation of a metal foil in front of the target face on which the electron beam is incident.

Let us consider qualitatively the physical nature of VCR in the case of oblique flight of a charged particle near a dielectric target. If the relativistic charged particle moves in vacuum ($n_1 = 1$) in the vicinity of a dielectric medium ($n_2 \neq 1$) at a constant velocity, electromagnetic radiation associated with this particle temporarily polarizes the medium in the vicinity of its trajectory (in our case, maximum polarization of atoms of the medium is observed at the interface between the two media). Thus, the oscillations of the molecules of the medium induced by the electromagnetic field of the charged particle become emitters of electromagnetic waves. In the general case, the waves emitted by the molecules in all parts of the interface between the two media interfere so that the intensity of the resultant field at a point located at a certain distance from the interface is zero.

If the velocity of a charged particle exceeds the phase velocity of light in the medium, the phases of

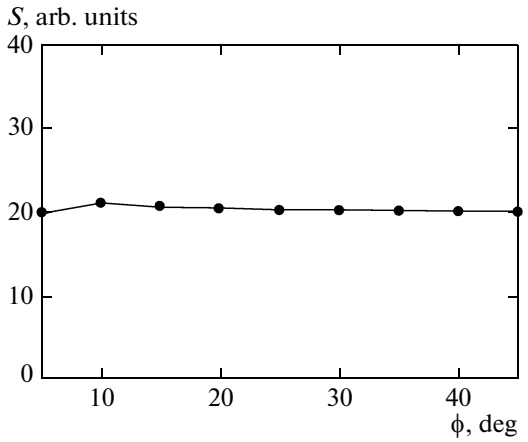

Fig. 8. Dependence of the total VCR intensity S on wedge angle ϕ. Parameters are $\gamma = 12$, $\sqrt{\varepsilon} = 1.41$, $b = 15$ mm, $l = 45\sqrt{2}$ mm, and $\lambda = 4$ mm.

elementary waves emitted from all parts of the interface may coincide at a certain point of observation, giving rise of a resultant field. It can be seen from the Huygens construction in Fig. 9 that this radiation can be observed only at a certain angle $\psi + \Theta$ relative to the perturbation propagation path at the interface between two media; it is the angle at which elementary waves from points P_1, P_2, and P_3 on perturbation propagation trajectory $A'B'$ are coherent and form plane front $B'C$ of the wave. This coherence takes place when a particle traverses distance AB during the time in which light traverses the distance from A' to C.

Thus, the coherence condition requires that the particle should traverse the distance from A to B over time interval Δt, while the radiation front during this time should traverse the segment from A' to C. If the particle velocity is βc, where c is the velocity of light, and if n_2 is the refractive index of the dielectric medium, we can write

$$A'B' = \frac{\beta c}{\cos\psi}\Delta t, \quad A'C = \frac{c}{n}\Delta t.$$

Hence it follows that

$$\cos(\psi + \Theta) = \frac{\cos\psi}{\beta n}. \tag{17}$$

This relation is the main result; it can be seen that for $\psi = 0$, this relation transforms to the well-known Vavilov–Cherenkov condition.

To confirm our arguments, let us compare the dependences of the VCR propagation angle on the angle of rotation of the target (Fig. 10). Curve *1* in Fig. 10 was obtained by the polarization current method (the radiation generation diagram is shown in Fig. 1), curve *2* was obtained using formula (17) and the Snell law. It should be noted that the curves in Fig. 10 completely coincide in the range of negative values of target rotation angle ψ; for positive angles, the slight difference observed in the behavior of the curves can be explained by the effect of the DR peak since for larger values of ψ, the VCR intensity becomes commensurate with the intensity of diffraction radiation, and the peaks are partly superimposed.

An additional proof of the effect considered here would be comparison of the spectral-angular distributions of VCR generated by wedge-shaped targets with different volumes. Figure 11 shows the diagram of generation of polarization radiation from a double target.

Performing calculations analogous to those carried out earlier for polarization radiation from a dielectric wedge, we arrive at the following expression for the intensity of polarization radiation in the forward direction:

$$\frac{d^2W}{d\omega d\Omega} = \frac{e^2\beta^2}{4\pi^2 c}\frac{\cos^2(\theta'-\alpha)}{|P|^2}\left|\frac{\varepsilon-1}{\varepsilon}\right|^2\left|1-\exp\left[-ia\frac{\omega}{\beta c}(P+\Sigma\cot\phi)\right]-\frac{P\exp\left[ia\frac{\omega}{\beta c}\Sigma\cot\phi\right]}{P+\Sigma\cot\phi}\right.$$

$$\left.+\frac{P^2+\Sigma^2\cot^2\phi}{P^2-\Sigma^2\cot^2\phi}\exp\left[-ia\frac{\omega}{\beta c}P\right]-\frac{\Sigma\cot\phi\exp\left[-ia\frac{\omega}{\beta c}\Sigma\cot\phi\right]}{P-\Sigma\cot\phi}\right|^2$$

$$\times\left\{\left|\frac{\varepsilon}{\varepsilon\cos(\theta'-\alpha)+\sqrt{\varepsilon-\sin^2(\theta'-\alpha)}}\right|^2\left|\cos\alpha(\gamma^{-1}\sin(\theta'-\alpha)-iK\cos\varphi\sqrt{\varepsilon-\sin^2(\theta'-\alpha)})\right.\right.$$

$$\left.+\sin\alpha(iK\sin(\theta'-\alpha)+\gamma^{-1}\cos\varphi\sqrt{\varepsilon-\sin^2(\theta'-\alpha)})-\gamma\beta\sin(\theta'-\alpha)\sqrt{\varepsilon-\sin^2(\theta'-\alpha)}\sin^2\varphi\right|^2 \tag{18}$$

$$+\left|\frac{\sqrt{\varepsilon}}{\cos(\theta'-\alpha)+\sqrt{\varepsilon-\sin^2(\theta'-\alpha)}}\right|^2(\gamma\sin\varphi)^2(\sin^2(\theta'-\alpha)+\left|\sqrt{\varepsilon-\sin^2(\theta'-\alpha)}\right|^2)$$

$$\left.\times[1-\beta^2\cos^2(\theta'-\alpha)+2\beta\gamma^{-2}\sin\alpha\sin(\theta'-\alpha)\cos\varphi-\gamma^{-2}\sin^2\alpha(K^2-\gamma^2)]\right\}$$

$$\times\frac{\exp\left[-2\frac{\omega}{\gamma\beta c}(h+a\cot\phi)K\cos\alpha\right]}{K^2[1-\beta^2\cos^2(\theta'-\alpha)+\beta^2\sin^2\alpha(1-\sin^2(\theta'-\alpha)\sin^2\varphi)+2\beta\sin\alpha\sin(\theta'-\alpha)\cos\varphi]}.$$

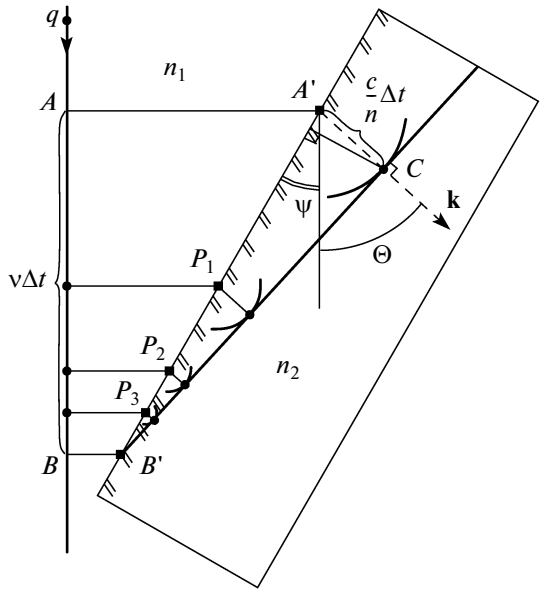

Fig. 9. Huygens construction illustrating the generation of coherent radiation.

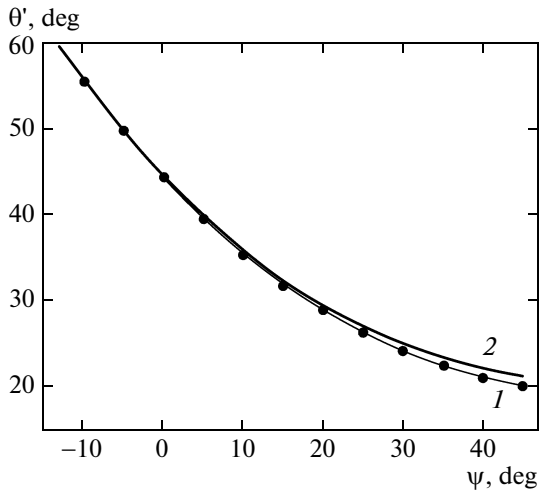

Fig. 10. Dependences of the angle of VCR propagation on the angle of rotation of the target relative to the charged particle trajectory: calculated using to polarization current method (diagram of generation is shown in Fig. 1) (*1*) and in accordance with formula (17) and Snell law (*2*). Parameters are $\sqrt{\varepsilon} = 1.41$, $b = 15$ mm, $\phi = \pi/4$, $a = 45$ mm, and $\lambda = 4$ mm.

This expression describes both DR and VCR. As in the previous case, the latter radiation corresponds to the main intensity pole

$$\left|\cos\alpha - \beta\sqrt{\varepsilon - \sin^2(\theta' - \alpha)} + i\gamma^{-1}K\sin\alpha\right| \longrightarrow 0$$

and the displacement pole determined by the geometry of the target under investigation.

The results of theoretical analysis are shown in Figs. 12 and 13. Comparison of the spectral-angular distributions of polarization radiation generated by prismatic targets with different volumes leads to the conclusion that only the *AB* face of the target facing the trajectory of the charged particle participates in the VCR generation, while the remaining faces (*AC* and *BC*) are responsible for DR generation.

3. DISCUSSION OF RESULTS

In this work, we have reported on the results of theoretical investigation of VCR generated by a charged particle flying near prismatic targets with an arbitrary permittivity. Our results make it possible to draw the main conclusion concerning the origin of the effect in question: VCR is generated in the surface layer of the interface between two media closest to the particle trajectory (face *AB* in Fig. 1), and its intensity is determined by the length of this face. The second conclusion becomes a logical continuation of the first: the VCR angular distribution in the case when a charged particle moves past a dielectric target does not obey the well-known Vavilov–Cherenkov condition, but is mainly determined by the orientation of the emitting layer relative to the trajectory of the charged particle. Therefore, polarization radiation can be represented as radiation occurring in the surface layer of the target due to dynamic polarization currents induced by the field of charged particles flying past the target.

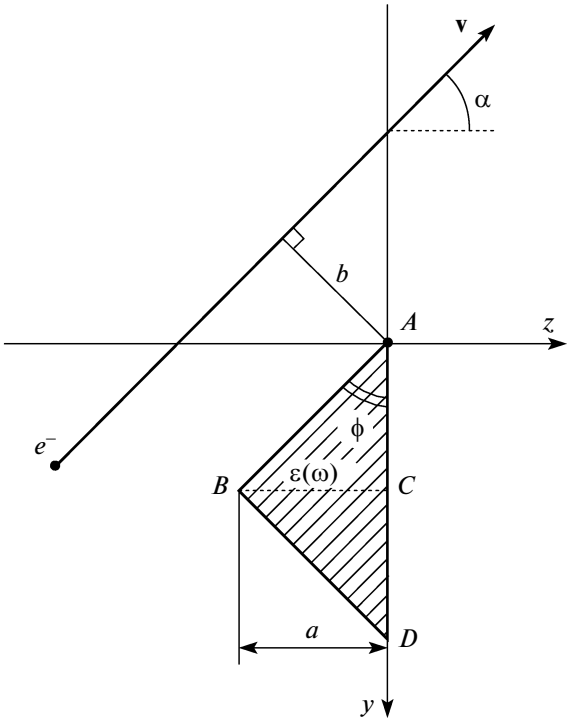

Fig. 11. Diagram of generation of polarization radiation by a charged particle moving uniformly near a double prismatic wedge.

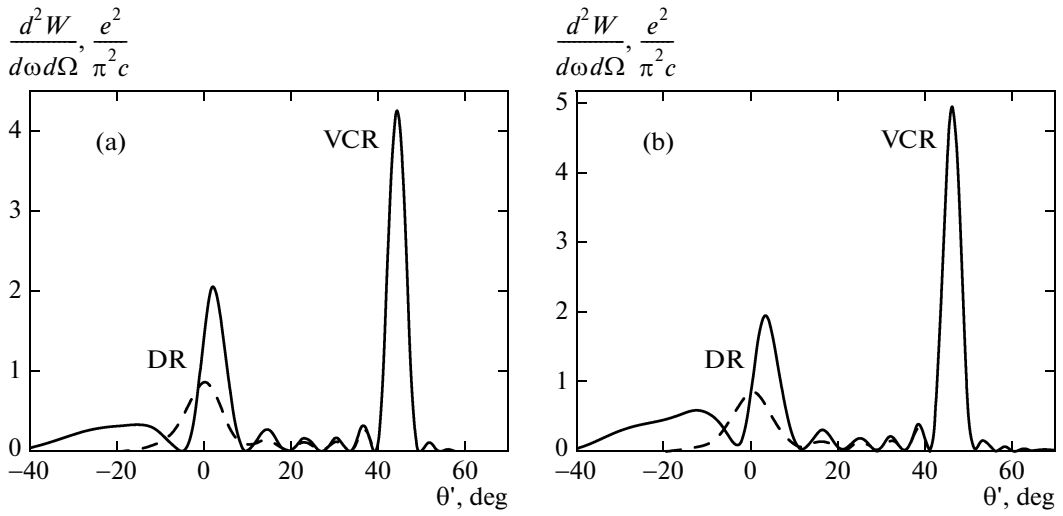

Fig. 12. Angular distributions of polarization radiation generated by a charged particle with energy $\gamma = 12$ moving past a dielectric wedge. Parameters are $\sqrt{\varepsilon} = 1.41$, $b = 15$ mm, $\phi = \pi/4$, $a = 45$ mm, and $\lambda = 4$ mm. Flight angle $\alpha = 45°$ (a) and 47° (b). Solid curves correspond to the double target and dashed curves correspond to the initial target.

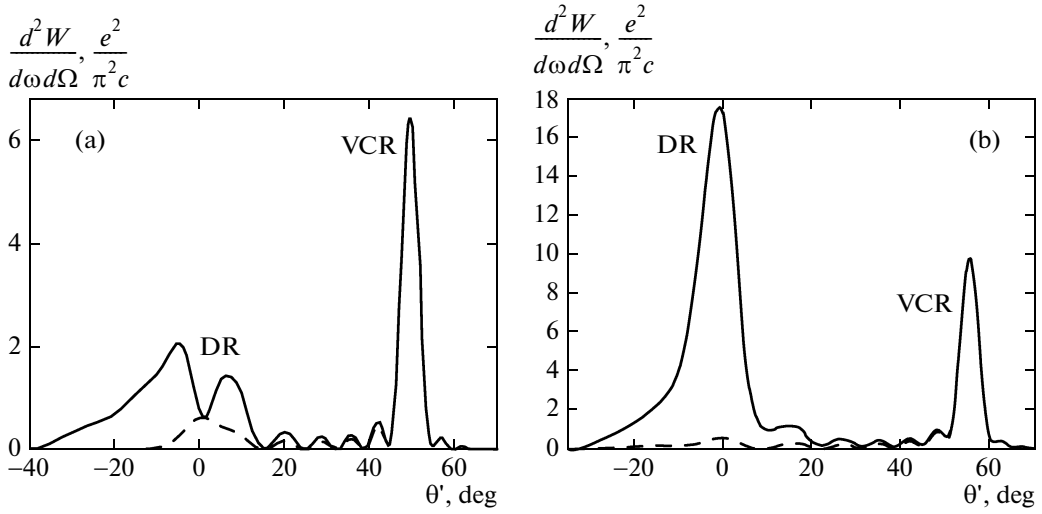

Fig. 13. Angular distributions of polarization radiation generated by a charged particle with energy $\gamma = 12$ moving past a dielectric wedge. Parameters are $\sqrt{\varepsilon} = 1.41$, $b = 15$ mm, $\phi = \pi/4$, $a = 45$ mm, and $\lambda = 4$ mm. Flight angle $\alpha = 50°$ (a) and 55° (b). Solid curves correspond to double target and dashed curves correspond to the initial target.

It should be noted that our results have a number of limitations associated with geometrical conditions as well as the approach used in this article for calculating the characteristics of polarization radiation. The application of Fresnel formulas (13) requires that the wedge face length $a/\tan\phi$ be much larger than the wavelength of the emitted radiation: $a/\tan\phi$. If the condition $a/\tan\phi \gg \lambda$ is satisfied, the output face of the prism can be assumed infinitely large, and the effect of the edges on the characteristics of radiation can be disregarded. Nor do Fresnel coefficients (13) allow us to consider possible multiple rereflections of polarization radiation inside the prism. Another equally important constraint is the condition imposed by the target geometry, which can be written in a very simple form: $0 < \phi < \pi/2$. However, this condition is not violated upon an increase in the prism volume if we add an analogous segment to the initial prism (see, for example, Fig. 11).

ACKNOWLEDGMENTS

The authors thank A.P. Potylitsyn, G.A. Naumenko, and D.V. Karlovets for support and valuable remarks.

A significant part of this research was supported financially by the Ministry of Education and Science of the Russian Federation (state contract no. 14V37.21.0775 and program "Nauka" no. 2.1799.2011). We would also like to acknowledge the Russian Foundation for Basic Research (grant no. 14-02-31642-mol_a).

REFERENCES

1. V. L. Ginzburg and I. M. Frank, Dokl. Akad. Nauk SSSR **56**, 699 (1947).
2. A. P. Potylitsyn, S. Yu. Gogolev, D. V. Karlovets, Yu. A. Popov, L. G. Sukhikh, G. A. Naumenko, and M. V. Shevelev, in *Proceedings of the First International Particle Accelerator Conference (IPAC'10), Kyoto, Japan, May 23–28, 2010* (Kyoto, 2010), p. 1074.
3. K. Kan, T. Kondoh, T. Kozawa, K. Norizawa, A. Ogata, J. Yang, and Y. Yoshida, in *Proceedings of the Tenth European Workshop on Beam Diagnostics and Instrumentation for Particle Accelerators (DIPAC'2011), Hamburg, Germany, May 16–18, 2011* (Hamburg, 2011), p. 368.
4. M. V. Shevelev, G. A. Naumenko, A. P. Potylitsyn, Yu. A. Popov, and L. G. Sukhikh, Nuovo Cimento Soc. Ital. Fis. **34** (4), 297 (2011).
5. T. Takahashi, Y. Shibata, K. Ishi, M. Ikezawa, M. Oyamada, and Y. Kondo, Phys. Rev. E: Stat. Phys., Plasmas, Fluids, Relat. Interdiscip. Top. **62**, 8606 (2000).
6. A. P. Potylitsyn, Yu. A. Popov, L. G. Sukhikh, G. A. Naumenko, and M. V. Shevelev, J. Phys.: Conf. Ser. **236**, 012025 (2010).
7. V. V. Vorobev and A. V. Tyukhtin, J. Phys.: Conf. Ser. **357**, 012006 (2012).
8. A. M. Cook, R. Tikhoplav, A. Y. Tichitsky, G. Travish, O. B. Williams, and J. B. Rosenzweig, Phys. Rev. Lett. **103**, 095003 (2009).
9. C. Jing, A. Kanareykin, J. G. Power, M. Conde, W. Liu, S. Antipov, P. Schoessow, and W. Gai, Phys. Rev. Lett. **106**, 164802 (2011).
10. B. M. Bolotovskii, Sov. Phys.—Usp. **4**, 781 (1961).
11. S. R. Arzumanyan, J. Phys.: Conf. Ser. **357**, 012008 (2012).
12. K. V. Lekomtsev, M. N. Strihanov, and A. A. Tishchenko, J. Phys.: Conf. Ser. **336**, 012023 (2010).
13. M. I. Ryazanov and I. S. Tilinin, Sov. Phys. JETP **44** (6), 1092 (1976).
14. D. V. Karlovets and A. P. Potylitsyn, JETP Lett. **90** (5), 326 (2009).
15. D. V. Karlovets, J. Exp. Theor. Phys. **113** (1), 27 (2011).
16. K. O. Kruchinin and D. V. Karlovets, Russ. Phys. J. **55** (1), 9 (2012).
17. M. I. Ryazanov, *Electrodynamics of Continuous Media* (Nauka, Moscow, 1984) [in Russian].
18. L. D. Landau and E. M. Lifshitz, *Course of Theoretical Physics*, Volume 8: *Electrodynamics of Continuous Media* (Butterworth–Heinemann, Oxford, 2004; Fizmatlit, Moscow, 2005).
19. M. Shevelev, G. Naumenko, A. Potylitsyn, and Y. Popov, J. Phys.: Conf. Ser. **357**, 012020 (2012).

Translated by N. Wadhwa